Stability of algebraically unstable dispersive flows

Kristina R. King,[1] Steven J. Weinstein,[2] Paula M. Zaretzky,[2]
Michael Cromer,[1] and Nathaniel S. Barlow[1,*]

[1]*School of Mathematical Sciences, Rochester Institute of Technology, Rochester, New York 14623, USA*
[2]*Department of Chemical Engineering, Rochester Institute of Technology, Rochester, New York 14623, USA*

A largely unexplored type of hydrodynamic instability is examined: long-time algebraic growth. Such growth is possible when the dispersion relation extracted from classical stability analysis indicates neutral stability. A physically motivated class of partial differential equations that describes the response of a system to disturbances is examined. Specifically, the propagation characteristics of the response are examined in the context of spatiotemporal stability theory. Morphological differences are identified between system responses that exhibit algebraic growth and the more typical case of exponential growth. One key attribute of predicted algebraically growing solutions is the prevalence of transient growth in almost all of the response, with the long-time growth occurring asymptotically at precisely one wave speed.

I. INTRODUCTION

The central aim of hydrodynamic stability theory is to determine whether disturbances to a fluid generate responses that grow or decay. This analysis is performed by tracking the response of the flow to perturbations through its governing equations and boundary conditions. For flows such as those found in thin film coating processes, for example, linearized equations are often a starting point for analysis, since even small perturbations to a thin film may make products unsalable due to tight uniformity constraints [1]. In these cases, the linear hydrodynamic stability of the underlying flow is relevant, and the precise manner in which the film responds is essential in practice; key features of a response includes its growth rate, breadth, and speed. For processes in which a flow may be adequately described by a linear partial differential equation (PDE), linear temporal modal stability analysis (henceforth referred to here as "modal analysis") is typically used to assess the stability of the flow, which assumes that the response to an arbitrary disturbance may be described by the superposition of fundamental modes.

To examine the growth in time, t, of the response h propagating in the x direction and starting from arbitrary nonzero initial conditions, a modal analysis proceeds by substituting the normal-mode form $h = e^{i(k_r x - \omega t)}$ into the governing PDE and examining the character of $\omega_{i,\,max}$, which is the maximum imaginary part of a generally complex frequency ω taken with respect to k_r, which is the real part of a generally complex wave number k. The system is linearly stable if $\omega_{i,\,max} < 0$ or linearly unstable if $\omega_{i,\,max} > 0$ over the interval $-\infty < k_r < \infty$. In the case where $\omega_{i,\,max} = 0$ over this interval, there is neither temporal growth nor decay, and the flow is termed "neutrally stable," a definition that will be used throughout this paper. This characterization assumes that the examination of individual modes is sufficient to characterize system stability. However, there are several neutrally stable flows in the literature [2–4] whose corresponding PDEs admit solutions that decay algebraically (typically like $t^{-1/2}$), shown through the method of stationary phase or steepest descent in a long-time asymptotic analysis [5,6]. For our proposed work, we are interested in the less-understood case of algebraic growth (i.e., perturbations that grow as t^s, $s > 0$). Since the introduction of modal analysis by Lord Rayleigh (1880) [7], the prospect of long-time nonexponential growth has been seldom mentioned and rarely investigated even in the context of nonmodal stability analysis.

---

*nsbsma@rit.edu

"Nonmodal" refers to analyses that, in general, determine stability through the examination of solution structure not captured by the individual modes or eigenvalues of the system [8]. One way in which algebraic growth can occur in a nonmodal analysis is through a *nonnormal* coefficient matrix $\mathbf{A}$ with eigenvalues λ, when the governing differential equation(s) are discretized in space and written as a time dependent system in matrix form. If $\mathbf{A}$ is nonnormal, the possibility exists that $\mathbf{A}$ is not diagonalizable, and a generalized eigenvector may be required to form a solution. This makes possible solutions that contain the form $t^n e^{\lambda t}$, where n is a positive integer. Even in the case where the real part of λ is negative, this form indicates that short-time transient growth occurs due to the t^n term. Short-time growth associated with the matrix $\mathbf{A}$ is often examined through its "pseudospectra" instead of its eigenvalues [8] via methods described in Refs. [9,10]. However, for both normal or nonnormal systems, the largest nonzero real eigenvalue of $\mathbf{A}$ dominates as $t \to \infty$, and thus normal and nonnormal stability analyses are equivalent in this limit. For systems where the real components of the eigenvalues of $\mathbf{A}$ are zero, long-time algebraic growth becomes a possibility. In the plasma field, "secular" instabilites arising from nonnormal operators have been observed [11–13], where a perturbation grows like t^n as $t \to \infty$ with n being an integer. Note that a normal system can also incur long-time algebraic growth. In fact, the linear operators discussed in this work are classified as normal, and the resulting algebraic growth is not restricted to integer powers in t.

An early example of normal yet nonmodal analysis is found in the work of Case (1960) [14], who examined the Rayleigh equation that governs inviscid plane Coette flow and, via asymptotic integral methods, showed an algebraic decay in the velocity field of order $1/t$ in the long-time limit. Emphasis here was placed on the examination of the *continuum* of modes, as the result cannot be derived by examining individual modes. The first published normal system exhibiting long-time algebraic growth was found in a Rayleigh equation for stratified shear flows [15]. Here, integral methods were applied to a normal system to predict a convective instability that grows algebraically, with a growth rate that depends on flow parameters. In the field of plasma instabilities, Rayleigh's equation (in cylindrical coordinates) was examined [16–19] and shown to lead to a $t^{1/2}$ growth. This same type of instability arose in an asymptotic analysis and numerical simulation of hurricane-like vortices [20].

More recently, long-time algebraic growth has been discovered in two classical fluid mechanics problems: (1) antisymmetric disturbances in a planar liquid sheet moving through an ambient quiescent gas for a range of Weber numbers, We (a parameter providing the relative magnitude of inertial to surface tension forces), and (2) symmetric disturbances in a liquid sheet in the absence of ambient gas for any We. The former is governed by a nonanalytic dispersion relation and grows as $t^{1/3}$ (introduced in Ref. [21], disputed in Ref. [22], and resolved in Ref. [23]). The latter is governed by the following nondimensional PDE [24]:

$$\frac{\partial^2 h}{\partial t^2} + \frac{\partial^2 h}{\partial x^2} + 2\frac{\partial^2 h}{\partial x \partial t} + \frac{1}{\text{We}}\frac{\partial^4 h}{\partial x^4} = 0, \quad -\infty < x < \infty, \quad t \geqslant 0. \tag{1}$$

For the above case, modal analysis indicates neutral stability, which implies that h neither grows (exponentially) nor decays (exponentially) as $t \to \infty$. This, however, does not correctly characterize the stability of the PDE. If all initial conditions in the above are imposed as impulses, it has been shown analytically [23] that the disturbance amplitude h grows in the x direction like $t^{1/2}$ in the long-time limit (see Fig. 1). In the current work, we examine a generalized form of the above PDE in order to explore its nonstandard nature.

One explanation for instability when modal analysis fails (i.e., the analysis predicts stability or neutral stability) is that nonlinear effects occur before stabilization is possible. The failure of some modal analyses may, in fact, be due to unrecognized occurrences of algebraic growth within the confines of linear theory. As shown in Fig. 1, the algebraically growing response contains attributes shared with solutions that have exponentially growing modes, such as a contiguous growing region surrounding the location of maximum growth (i.e., $h_{\max}$ in Fig. 1). However, the underlying mathematical features of the response are distinctly different. The focus of this paper is to examine the relevant properties of an algebraically growing response, such as the one shown in Fig. 1.
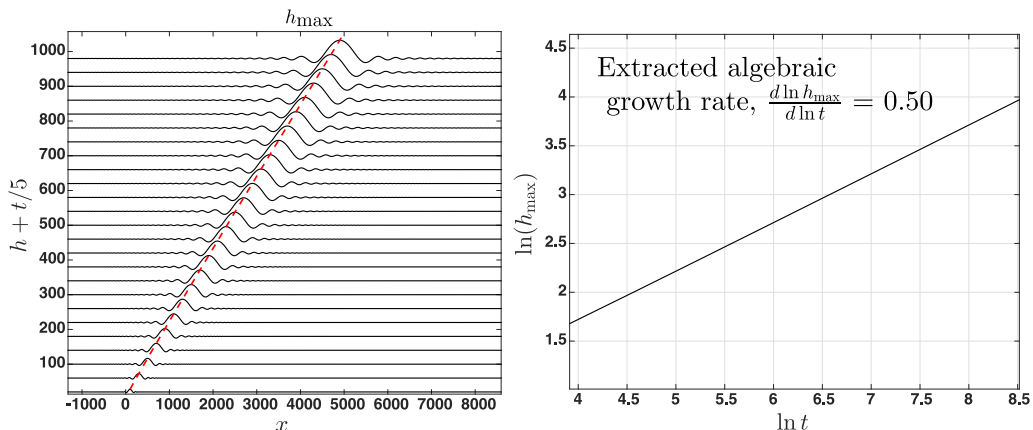
FIG. 1. Fourier series solution of Eq. (1) with $N = 4000$ Fourier modes and $1/\text{We} = 50$, indicating agreement (here to two significant figures) with the analytical prediction of a response that grows as $t^{1/2}$ [23]. The dashed line is the locus of the maxima of the response, $h_{\max}$, whose growth rate is shown in the adjacent figure.

The paper is organized as follows. In Sec. II the symmetric liquid sheet wave equation [Eq. (1)] is generalized to a class of PDEs whose modal analysis indicates neutral stability, but whose solution is, in fact, algebraically unstable. Standard techniques of spatiotemporal stability analysis are applied to this class of PDEs to examine its stability and a general form is extracted for the rate of algebraic growth. In Sec. III the physical differences between algebraically and exponentially growing responses in a fluid (or any dispersive media) are examined, and the key findings of this work are summarized in Sec. IV.

II. ALGEBRAIC INSTABILITY

Equation (1) belongs to a class of physically relevant, normal skew-symmetric [25] PDEs whose modal analysis indicates neutral stability but whose solution exhibits algebraic growth:

$$\frac{\partial^2 h}{\partial t^2} + c^2 \frac{\partial^2 h}{\partial x^2} + 2c \frac{\partial^2 h}{\partial x \partial t} + (-1)^n \alpha^2 \frac{\partial^{2n} h}{\partial x^{2n}} = A\delta(x)\delta(t),$$

$$h(x,0) = h_0 \delta(x) \quad \text{and} \quad \frac{\partial h}{\partial t}(x,0) = v_0 \delta(x) \quad \text{for all } x, \tag{2}$$

$$h \to 0 \quad \text{as} \quad x \to \pm\infty \quad \text{for all } t.$$

In Eq. (2), h is the system response; c and $\alpha \neq 0$ are real-valued parameters; A is an impulsive forcing amplitude; h_0 and v_0 are the amplitudes of delta function perturbations $\delta(x)$ of the initial conditions; and $n \geqslant 2$ is an integer. In the derivation of response evolution equations from first principles, different values of n may arise. For example, in lubrication theory, the linearized governing equations for a deformable boundary have a second order spatial derivative in pressure embedded in the evolution equation [26]. This pressure has a second order spatial derivative in height for tension effects [23,26] and/or a fourth order spatial derivative in height for elastic effects [27]. When inserted into an evolution equation such as Eq. (2), these translate to $n = 2$ and 3, respectively.

Three types of delta function perturbations with amplitudes A, h_0, and v_0 are included in Eq. (2) so that their effect may be tracked through the stability analysis. When $h_0 = v_0 = 0$, the system provides the well-known "impulse response" (i.e., Green's function) solution to the PDE, which is typically used to determine the spatiotemporal stability of a system [28,29]. Such a disturbance invokes nonzero amplitudes of every Fourier mode of the homogeneous version of Eq. (2), and all

responses to forcing in Eq. (2) can be obtained through a convolution of the imposed forcing and the Green's function [30]. From a physical perspective, the delta function is a judicious choice of forcing because it enables one to initiate a disturbance at a single instance in time and space without obscuring the subsequent response of the underlying media [31]. In experiments, delta function forcing can be approximated by the electro-capillarity blade technique shown in Ref. [32]. The delta function may be thought of as an idealized Gaussian [33]. If one were to use an actual Gaussian (or another localized continuous function) to initiate the disturbances examined in this paper, the long-time asymptotic stability result would be identical [4,23]. In thin liquid sheets, for example, the delta function may be motivated as an idealized Gaussian pressure disturbance in the dynamic boundary condition across the surface of the sheet [34]. This leads to a delta function forcing term in the governing PDE or (equivalently, for the liquid sheet problem) a delta function initial condition in $\frac{\partial h}{\partial t}$. Alternatively, one may disturb a liquid sheet through an idealized Gaussian "pluck" to the surface, as done in Refs. [23,24]. For completeness, initial impulse perturbations in h and $\frac{\partial h}{\partial t}$ having respective amplitudes h_0 and v_0 are similarly included here to determine the effect of the type of disturbance on the system response.

Although problems such as Eq. (2) can be solved completely using a Fourier series expansion [4,23,34], such an approach does not provide precise growth rates, and thus conclusions regarding system stability, as well as the structure of the response, may be obscured. Spatiotemporal stability theory enables one to explicitly extract the details of growth through asymptotic analysis [35,36]. Following the typical approach taken to examine the spatiotemporal stability of a system [28–30], the integral solution of Eq. (2) is obtained by first taking the successive Fourier and Laplace transforms (in space and time, respectively) such that the partial differential equation in $h(x,t)$ becomes an algebraic equation in $\mathcal{H}(k,s)$. It is implicit in this notation that x transforms to k, t transforms to s, and h transforms in aggregate to $\mathcal{H}$. After solving for the doubly transformed variable $\mathcal{H}$, one may then take the subsequent inverse Fourier and Laplace transforms to recover $h(x,t)$. Using the standard convention followed in wave problems of rotating the Laplace contour such that $s = -i\omega$, the integral solution of Eq. (2) becomes

$$h(x,t) = \frac{1}{4\pi^2} \int_{-\infty}^{\infty} \int_{-\infty+i\tau_0}^{\infty+i\tau_0} \frac{f(k,\omega)}{D(k,\omega)} e^{i(kx-\omega t)} \, d\omega \, dk, \tag{3}$$

where

$$f(k,\omega) = A + v_0 + ih_0(2ck - \omega), \tag{4}$$

$$D(k,\omega) = \alpha^2 k^{2n} - (ck - \omega)^2, \tag{5a}$$

and $D(k,\omega) = 0$ is the dispersion relation that describes the relationship between the complex wave number $k = k_r + ik_i$ and complex frequency $\omega = \omega_r + i\omega_i$ in the flow governed by Eq. (2). In the above and all of the following, the subscripts r and i indicate real and imaginary components, respectively. Note that $D(k,\omega) = 0$ is easily obtained by substituting $h = e^{i(kx-\omega t)}$ into the homogeneous form of the governing PDE [here (2)] with no constraints applied. The parameter τ_0 in Eq. (3) is chosen such that the horizontal integration path in the ω_r-ω_i plane passes above all singularities in the integrand; this restriction is embedded in the inverse Laplace transform [37] and ensures that causality (no disturbance can arise prior to the time $t = 0$) is satisfied. The path of the Fourier inversion is taken to be along the k_r axis in Eq. (3), although any path in the domain of convergence of the transform may be chosen. The k_r axis is guaranteed to be a path of convergence based on its relationship to the discrete Fourier series that arises from a self-adjoint eigenvalue problem on a finite domain, where the eigenvalues are real [38].

The dispersion relation, $D(k,\omega) = 0$, given by Eq. (5a) may be written as

$$\omega_\pm = ck \pm \alpha k^n. \tag{5b}$$

In Eq. (5b) it is clear that, for any n, $\omega_i = 0$ for all k_r. Thus, the class of PDEs given by Eq. (2) are neutrally stable. Note that the definition in Sec. I requires only that the maximum growth be

zero (i.e., for one mode) for the system to be neutrally stability, whereas here all modes have zero growth. The assessment of nonmodal stability that follows requires careful asymptotic analysis of the integrals in Eq. (3).

The double integral in Eq. (3) is evaluated through one integration in ω (Laplace integral) and one in k (Fourier integral), which may be done in any order. As is usually the case, one order is arguably easier than another, but the answers will be equivalent, provided that the order does not affect the existence of the integrals. The first integration (in ω or k) is carried out by applying the residue theorem, which leads to the substitution of either $k(\omega)$ roots or $\omega(k)$ roots of $D(k,\omega) = 0$ in to the argument of the exponential in Eq. (3). Although both approaches have been taken in the literature to analyze the response to an initial disturbance [28,29,39], performing the Laplace integral first is generally easier [4,23]. This is certainly the case for Eq. (3), given that the number of ω roots is known while the number of k roots depends on the value of n; hence, it is easier to write $\omega(k)$ (Laplace inversion first) rather than $k(\omega)$ (Fourier inversion first).

Evaluating the inner (Laplace) integral of Eq. (3) by the method of residues results in the Fourier integral solution:

$$
\begin{aligned}
h(x,t) = {} & \frac{-\mathrm{i}(A + v_0)}{4\pi\alpha} \int_{-\infty}^{\infty} \frac{e^{\mathrm{i}[kx-\omega_-(k)t]} - e^{\mathrm{i}[kx-\omega_+(k)t]}}{k^n} \, dk \\
& + \frac{ch_0}{4\pi\alpha} \int_{-\infty}^{\infty} \frac{e^{\mathrm{i}[kx-\omega_-(k)t]} - e^{\mathrm{i}[kx-\omega_+(k)t]}}{k^{n-1}} \, dk \\
& + \frac{h_0}{4\pi\alpha} \int_{-\infty}^{\infty} \{ e^{\mathrm{i}[kx-\omega_-(k)t]} - e^{\mathrm{i}[kx-\omega_+(k)t]} \} \, dk.
\end{aligned}
\tag{6}
$$

Typically, one would decompose Eq. (6) into six integrals with the goal of applying asymptotic analysis to each exponential function separately (for example, using the method of stationary phase). However, the denominators of the integrands in Eq. (6) have poles of order n and $n-1$ at $k = 0$ that prevent a standard approach. Although it is a natural inclination to interpret these six integrals as principal values, it is only when the poles are of odd order that the principal values exist. Since the original problem is well posed and a unique solution is expected for *any* n, one anticipates that the integrand may be rewritten in a way that the poles are eliminated, i.e., they are removable singularities. Substituting Eq. (5b) into Eq. (6) leads to

$$
\begin{aligned}
h(x,t) = {} & \frac{A + v_0}{2\pi\alpha} \int_{-\infty}^{\infty} \frac{\sin(\alpha k^n t)}{k^n} e^{\mathrm{i}k(\frac{x}{t}-c)t} \, dk \\
& + \frac{\mathrm{i}ch_0}{2\pi\alpha} \int_{-\infty}^{\infty} \frac{\sin(\alpha k^n t)}{k^{n-1}} e^{\mathrm{i}k(\frac{x}{t}-c)t} \, dk + \frac{h_0}{2\pi\alpha} \int_{-\infty}^{\infty} \cos(\alpha k^n t) e^{\mathrm{i}k(\frac{x}{t}-c)t} \, dk.
\end{aligned}
\tag{7}
$$

Note that the above integrals can be obtained in a more straightforward manner by taking the Fourier transform of Eq. (2), solving the resulting ODE with respect to t, and then taking the inverse Fourier transform (see Appendix A). Here the standard spatiotemporal stability analysis approach is used in order to bridge with previous analyses and to highlight the care with which integrands need to be written to ensure that removable singularities are handled appropriately. Normally, individual exponential terms in Eq. (6) enable direct asymptotic analysis that leads to a description of the (exponential) growth and breadth of a system response [28,30]. For algebraic growth, however, the removable singularities necessitate that a modified approach be taken; the full details of the methodology is provided in Appendix B.

In what follows, the algebraic growth rate that characterizes the system response is determined analytically. Note that the exponential arguments in Eq. (7) are written to mimic the approach used in stationary phase or saddle point analysis; the quantity t is factored out, and the "velocity" quantity $\frac{x}{t}$ is introduced. The integrals in Eq. (7) are to be evaluated for fixed values of x/t; this aspect of the analysis is shared with the saddle point approach for exponentially growing waves [3]. Before continuing, it is useful to decompose the remaining exponentials of Eq. (7) into sines and cosines,

since identities for such integrals are readily available. This leads to six integrals: three with even integrands and three with odd integrands, which may be rewritten in compact form as follows:

$$h(x,t) = \frac{A + v_0}{\pi\alpha} \int_0^\infty \frac{\sin(\alpha k^n t)\cos\left[k\left(\frac{x}{t} - c\right)t\right]}{k^n}\,dk$$

$$- \frac{ch_0}{\pi\alpha} \int_0^\infty \frac{\sin(\alpha k^n t)\sin\left[k\left(\frac{x}{t} - c\right)t\right]}{k^{n-1}}\,dk$$

$$+ \frac{h_0}{\pi\alpha} \int_0^\infty \cos(\alpha k^n t)\cos\left[k\left(\frac{x}{t} - c\right)t\right]dk. \tag{8}$$

For $\frac{x}{t} = c$, Eq. (8) may be evaluated using the identities given by Eqs. (B3) and (B4) provided in Appendix B 1 to yield

$$h(x,t)|_{\frac{x}{t}=c} = \frac{\Gamma\left(\frac{1}{n}\right)\cos\left(\frac{\pi}{2n}\right)}{\pi\alpha^{1/n}}\left[\frac{A + v_0}{n-1}t^{1-\frac{1}{n}} + \frac{h_0}{n\alpha}t^{-\frac{1}{n}}\right], \tag{9}$$

which is exact for *all* t. For $\frac{x}{t} \neq c$, asymptotic analysis as $t \to \infty$ is used to evaluate the integrals in Eq. (8). Using the leading-order terms provided by the long-time asymptotic expansion of Eq. (8) given by Eq. (B17) in Appendix B 2, the solution for $\frac{x}{t} \neq c$ is given by

$$h(x,t)|_{\frac{x}{t}\neq c} \sim \left\{\frac{(A + v_0)\alpha^{\frac{1}{2n-2}}n^{\frac{2n-1}{2n-2}}}{\sqrt{2\pi(n-1)}\left|\frac{x}{t} - c\right|^{\frac{3n-2}{2n-2}}}t^{-1/2}\right\}\cos\left[(n-1)\left(\frac{\left|\frac{x}{t} - c\right|}{n}\right)^{\frac{n}{n-1}}\alpha^{\frac{1}{1-n}}t + \frac{\pi}{4}\right]$$

$$+ \left\{\frac{h_0}{\sqrt{2\pi(n-1)}\left|\frac{x}{t} - c\right|^{\frac{n-2}{2n-2}}(\alpha n)^{\frac{1}{2n-2}}}\left[\frac{cn}{\left(c - \frac{x}{t}\right)} + \frac{1}{\alpha}\right]t^{-1/2}\right\}$$

$$\times \cos\left[(n-1)\left(\frac{\left|\frac{x}{t} - c\right|}{n}\right)^{\frac{n}{n-1}}\alpha^{\frac{1}{1-n}}t - \frac{\pi}{4}\right]t^{-\frac{1}{2}} + O(t^{-1}), \quad t \to \infty. \tag{10}$$

If the system described by Eq. (2) is perturbed with all indicated disturbances included (i.e., $A + v_0 \neq 0$, $h_0 \neq 0$), then Eqs. (9) and (10) together describe an evolving response with a peak that travels at speed c and grows like $t^{1-1/n}$ as $t \to \infty$. Note that, for the class of problems described by Eq. (2), this asymptotic growth rate also holds for $h_0 = 0$ (with $A + v_0 \neq 0$).

The response at specific times, as given by the Fourier series solution to Eq. (2), is compared with the leading order asymptotic solution given by Eq. (10) in Fig. 2 for $n = 2$ and Fig. 3 for $n = 3$. All Fourier series solutions displayed in this paper are constructed on a periodic domain, following the approach given in Ref. [4]. In Figs. 2 and 3, note that only the peak grows as $t \to \infty$, since Eq. (9) describes a single amplitude (i.e., no x dependence) moving at speed c, and every portion of the response not moving at this speed adheres to Eq. (10), decaying like $t^{-1/2}$ as $t \to \infty$. This behavior is confirmed in Fig. 4 for $n = 2$ and Fig. 5 for $n = 3$, where peak and off-peak amplitudes of the Fourier series solution of Eq. (2) are plotted versus time for several fixed x/t values and compared with Eqs. (9) and (10). In the bottom plots of Figs. 4 and 5, the asymptotic solution given by Eq. (10) is shown to approach the Fourier series solution as $t \to \infty$ for a fixed x/t. Accordingly, the gap in the asymptotic solution seen in Figs. 2 and 3 is merely an indication that, along the collection of x/t rays within this gap, t is not yet large enough for the asymptotic behavior to be captured by Eq. (10). It is apparent, then, that the limit as $t \to \infty$ is not uniform in x/t as $x/t \to c$.

As can be seen in Figs. 2 and 3, growth appears to be spreading as opposed to being confined to a single peak moving at $x/t = c$. The growing response that we see is, in fact, mostly made of transient ("short"-time) growth, which, along any given ray $x/t \neq c$ will eventually damp as $t \to \infty$. Points
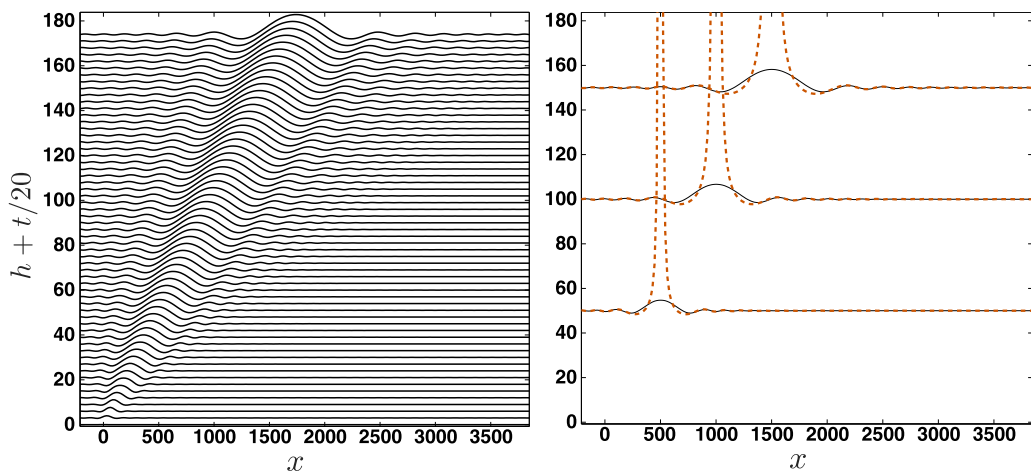
FIG. 2. Fourier series solution (solid curves) to Eq. (2) with $n = 2$ compared with leading-order asymptotic solution given by Eq. (10) (right, dashed curves). $\alpha = 5\sqrt{2}$, $c = 1$, $A = 0$, $h_0 = v_0 = 1$.

moving near the peak of the response at velocities closer to c will take a longer time to damp, as can be seen in Figs. 4 and 5.

The interplay between short-term growth and long-term damping for $x/t \neq c$ may be seen explicitly in the exact solution of (2) for $n = 2$. This solution is valid for any x/t and all t and is obtained by applying the integral identities given by Eqs. (B18)–(B20) (in Appendix B 3) to Eq. (8):

$$
h(x,t) = \frac{\left|\frac{x}{t} - c\right|}{2\alpha} \left[S\left(\frac{\left|\frac{x}{t} - c\right|}{2a^{\frac{1}{2}}} t^{\frac{1}{2}} \right) - C\left(\frac{\left|\frac{x}{t} - c\right|}{2a^{\frac{1}{2}}} t^{\frac{1}{2}} \right) \right] \left[A + v_0 - \frac{ch_0}{\left(\frac{x}{t} - c\right)} \right]
$$
$$
+ \frac{1}{\sqrt{\pi}} \cos\left[\frac{\pi}{4} - \frac{\left(\frac{x}{t} - c\right)^2 t}{2\alpha} \right] \left(\frac{A + v_0}{\sqrt{\alpha}} t^{1/2} + \frac{h_0}{2\alpha^{3/2}} t^{-1/2} \right). \tag{11}
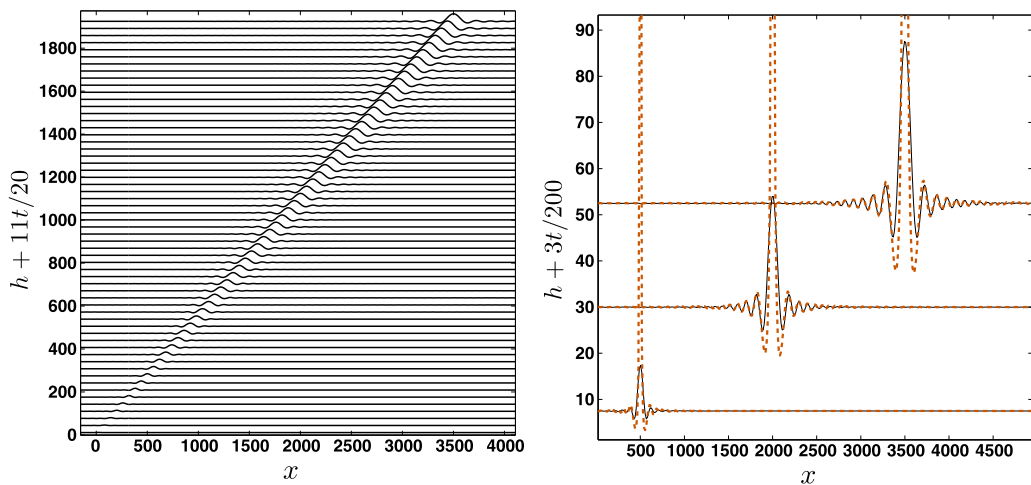$$

FIG. 3. Fourier series solution (solid curves) to Eq. (2) with $n = 3$ compared with leading-order asymptotic solution given by Eq. (10) (right, dashed curves). $\alpha = 5\sqrt{2}$, $c = 1$, $A = 0$, $h_0 = v_0 = 1$.
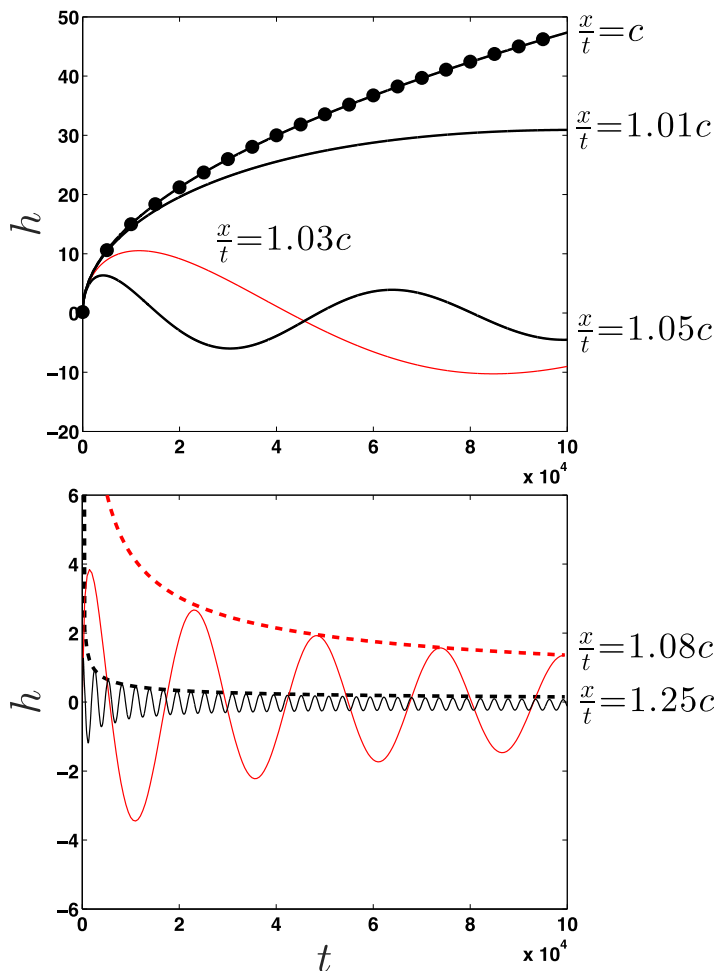
FIG. 4. Fourier series solution (solid curves) to Eq. (2) with $n = 2$ along specific x/t rays, compared with exact solution given by Eq. (9) (top, ●) along $x/t = c$ and envelopes of asymptotic solution [bracketed terms in Eq. (10)] (bottom, dashed curves) for $x/t \neq c$. $\alpha = 5\sqrt{2}$, $c = 1$, $A = 0$, $h_0 = v_0 = 1$.

In Eq. (11), $S()$ and $C()$ are Fresnel integrals given by Eq. (B19b). In the limit as $t \to 0$, the leading-order term in Eq. (11) contains no x/t dependence and is precisely the algebraic growth expression given by Eq. (9) (for $n = 2$). This effect can be seen in Fig. 4, where, if one examines the limit of small t for any x/t, the $x/t = c$ and $x/t \neq c$ solutions align and growth occurs at the same rate and with the same amplitude. As x/t moves away from c, decay overcomes growth more rapidly. The same behavior is observed for all n (e.g., see Fig. 5 for $n = 3$).

Choice of impulsive perturbation

Note that if $A + v_0 = 0$ and $h_0 \neq 0$ in Eq. (2), then Eqs. (9) and (10) indicate that the flow is algebraically stable and the response decays like $t^{-1/n}$. This is the type of solution presented in Ref. [24] (Fig. 3.7) for a liquid sheet governed by Eq. (2) (with $n = 2$, $c = 1$) and for an elastic beam response illustrated in Ref. [9] (Fig. 54.3) that is governed by Eq. (2) (with $n = 2$, $c = 0$). Thus, an impulse can be introduced to a system, either through A, v_0, or h_0, and this choice will affect the algebraic stability or instability of the response [34]. This is an important feature
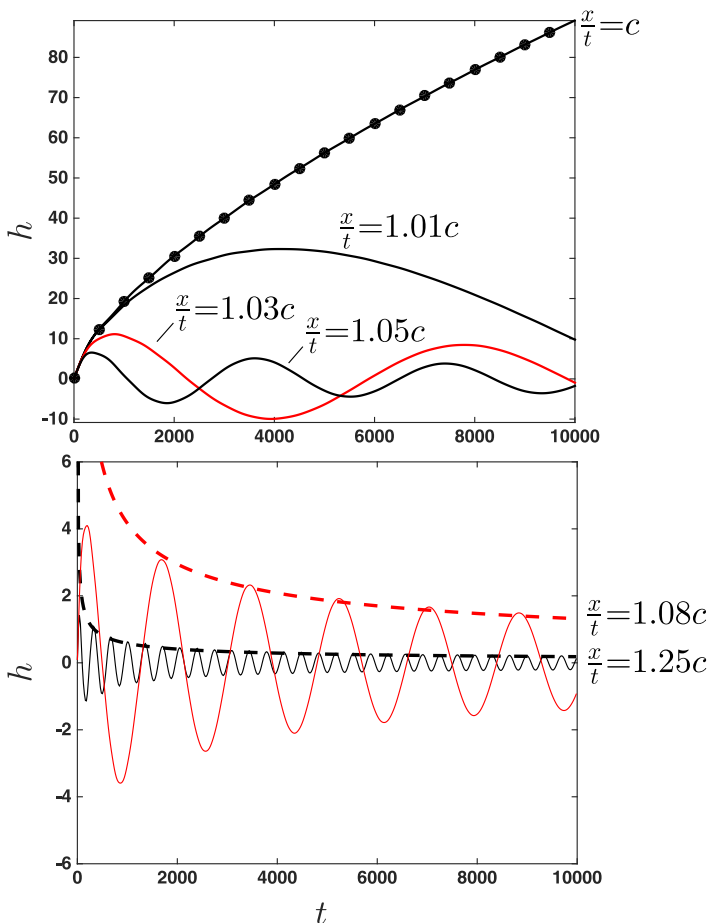
FIG. 5. Fourier series solution (solid curves) to Eq. (2) with $n = 3$ along specific x/t rays, compared with exact solution given by Eq. (9) (top, •) along $x/t = c$ and envelopes of asymptotic solution [bracketed terms in Eq. (10)] (bottom, dashed curves) for $x/t \neq c$. $\alpha = 5\sqrt{2}$, $c = 1$, $A = 0$, $h_0 = v_0 = 1$.

of the solution, and provides a cautionary note. A system is stable if its response decays for all possible disturbances. One must thus cast a "wide net" to ensure that all disturbances are captured in the system response. It appears that algebraically growing systems are particularly sensitive to the choice of initiating disturbance, as evidenced by the results above. By contrast, in the case of exponential instability, where temporal stability is determined exclusively through modal analysis (see Ref. [35] and Sec. III below), any type of impulsive initial condition and/or forcing will lead to the same long-time behavior. In the following section, we compare other aspects of exponential instabilities with algebraic instabilities.

III. COMPARISON OF ALGEBRAICALLY AND EXPONENTIALLY GROWING SYSTEM RESPONSES

In order to make a comparison between algebraic growth and the established features of exponential growth, the real parameter s is introduced as the algebraic growth rate for responses that grow like t^s as $t \to \infty$. For the class of PDEs described by Eq. (2), s is a *discontinuous* function of

x/t, as indicted in Eqs. (9) and (10):

$$s = \begin{cases} 1 - 1/n : & x/t = c \\ -1/2 : & x/t \neq c. \end{cases} \tag{12}$$

Note that, although s is discontinuous, transient growth and decay ensure that the waveform is, in fact, continuous, as elucidated in Figs. 2 and 3 and the surrounding discussion; we return to this point at the end of this section. The algebraic growth described above is in contrast with exponential growth like $e^{\sigma t}$ as $t \to \infty$. The exponential growth rate σ is obtained by applying the method of steepest descent to the Fourier integral solution [e.g., Eq. (6)] [6,40]. In this method, the argument of the exponential, $\mathrm{i}[k\frac{x}{t} - \omega(k)]t$, is expanded about the k value that maximizes the real part of the phase function $\phi = \mathrm{i}[k\frac{x}{t} - \omega(k)]$ for a fixed x/t. If the integration path is taken to pass through this saddle point k_s, the dominant portion of the leading order asymptotic behavior of the integral as $t \to \infty$ is then $e^{\sigma t}$, where $\sigma = \mathrm{Real}[\phi(k_s)]$. The continuous spectrum of saddles [41] associated with the continuous possible x/t values leads to an exponential growth rate σ that is a *continuous* function of x/t. For illustration, consider the impulsively perturbed linearized Ginzburg-Landau equation,

$$\frac{\partial h}{\partial t} + U\frac{\partial h}{\partial x} - \mu h - \gamma\frac{\partial^2 h}{\partial x^2} = A\delta(x)\delta(t),$$
$$h(x,0) = h_0\delta(x) \quad \text{for all } x, \tag{13}$$
$$h \to 0 \quad \text{as} \quad x \to \pm\infty \quad \text{for all } t,$$

typically used as a simple model for convectively and absolutely unstable responses in both open and closed fluid flows (see Refs. [29,42] and references therein). The real-valued parameters U, μ, and γ are used to describe convection, degree of instability, and diffusion, respectively. The solution and modal analysis of Eq. (13) (as written above in a simplified form) is given in Refs. [35,43]. The locus of saddle points for Eq. (13) is

$$k_s = \frac{\mathrm{i}}{2\gamma}\left[\frac{x}{t} - U\right], \tag{14a}$$

and the exponential growth rate associated with these saddles is

$$\sigma = \mu - \frac{1}{4\gamma}\left(\frac{x}{t} - U\right)^2. \tag{14b}$$

The character described above for exponential instabilities is a cornerstone of spatiotemporal linear stability analysis, where growing disturbances are classified as either convectively or absolutely unstable, depending on whether or not the response convects away from or persists at the location of the initial disturbance, respectively [28,30,44]. This distinction is important for any transport process where instabilities occur [45]. Using the nomenclature above, if one tracks along the stationary ray $x/t = 0$ in the response and discovers that it exponentially decays ($\sigma < 0$), then any instability will convect away from the initial location of the disturbance; this defines a convective instability [see Fig. 6(a)]. Alternatively, an absolutely unstable flow is described by governing equations that lead to exponential growth ($\sigma > 0$) for $x/t = 0$ [see Fig. 6(b)].

From a physical perspective, if a disturbance moves along a specific velocity within the growing response, it will grow at a specific exponential rate, and this will be associated with a specific wave number, k_s [see Eq. (14a)], which is a saddle point of the asymptotic analysis; note that this is a resultant wave number obtained by the superposition of underlying normal modes. Each k_s value lies in a continuous spectrum of other saddle points, as evidenced from Fig. 6. This growing packet is bounded by the x/t values V_+ and V_- where $\sigma = 0$, as shown in Fig. 6. Maximum growth occurs at $x/t = V_{\max}$, where $\sigma = \omega_{\mathrm{i,max}}$. Detailed examples that lead to this interpretation are given in Refs. [28,30,34]. For algebraically growing responses, the qualitative description of convective versus absolute instabilities holds, but some of the flow features are different and are now elucidated.
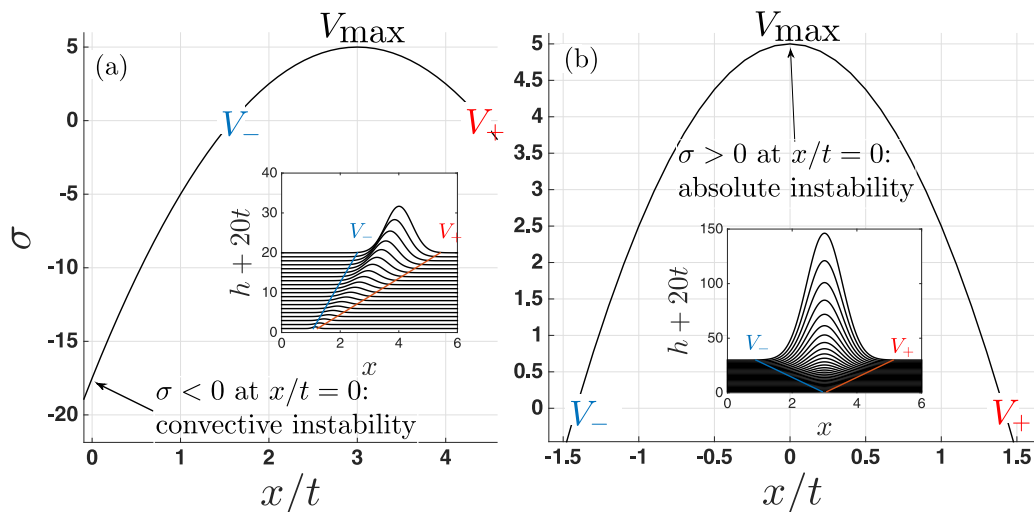
FIG. 6. Exponential growth rate σ along rays x/t for a flow described by the linear Ginzburg-Landau equation given by Eq. (13) with $\mu = 5$, $\gamma = 0.1$, $A = 0$, and $h_0 = 1$; (a) convective instability ($U = 3$); (b) absolute instability ($U = 0$). Insets show the Fourier series solution of Eq. (13).

In a σ versus x/t plot like Fig. 6 for the algebraically growing flow described by Eq. (2), the curve is a horizontal line $\sigma = 0$ for all x/t. Since there is no exponentially growing response, one cannot rely on locations of zero growth rate in the exponential to determine the characteristic rays that bound the system response, i.e., the rays $x/t = 0$, $V_{\max}$, V_+, and V_-. In order to make a relevant comparison to Fig. 6, Fig. 7 shows a graphical depiction of Eq. (12): the algebraic growth rate in Eq. (2) versus x/t. The convective or absolute instability classification is identical to that given above for exponential instabilities, if we replace σ with s. The insets of Fig. 7 showing convectively and
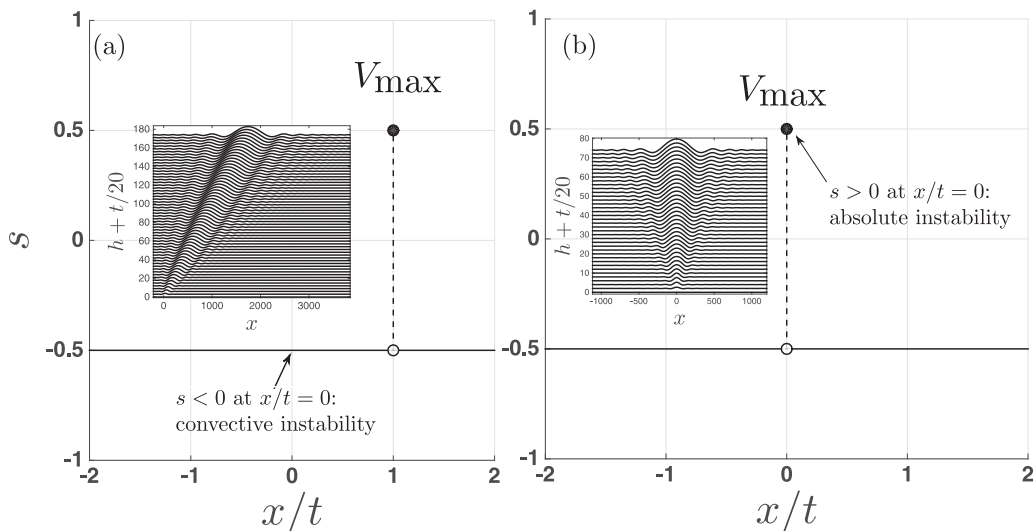

FIG. 7. Algebraic growth rate s along rays x/t for a flow described by Eq. (2) with $n = 2$, $\alpha = 5\sqrt{2}$, $A = 0$, and $h_0 = v_0 = 1$; (a) convective instability ($c = 1$) and (b) absolute instability ($c = 0$). Insets show the Fourier series solution of Eq. (2).
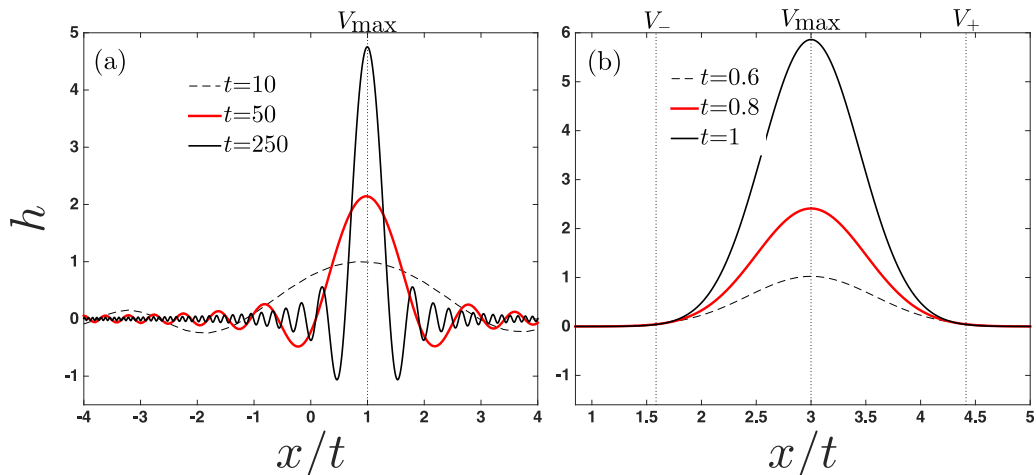
FIG. 8. Comparison between (a) algebraic and (b) exponential growth vs x/t. (a): Fourier series solution to Eq. (2) with $n = 2$, $\alpha = 5\sqrt{2}$, $c = 1$, $A = 0$, $h_0 = v_0 = 1$. Here $V_{max} = c$. (b): Fourier series solution to Eq. (13) with $\mu = 5$, $\gamma = 0.1$, $A = 0$, $U = 3$, $h_0 = 1$. Here $V_{max} = U$.

absolutely unstable algebraically growing waves look similar to the insets of Fig. 6 for exponentially growing waves. The algebraic growth even appears to have bounds upstream and downstream of the peak. However, the bounding rays exist only in the sense that $V_+ = V_{max} + \epsilon$ and $V_- = V_{max} - \epsilon$, where $\epsilon \to 0$ as $t \to \infty$; recall from Eqs. (9) and (10) that the only growing ray is $V_{max} = c$ as $t \to \infty$.

The features described above, which distinguish the algebraic growth exhibited by Eq. (2) from exponentially growing waves, becomes clear when viewed in a plot of h versus x/t, shown in Fig. 8 for each type of growth. An exponentially unstable packet is formed from a growing peak in a region of long-time growth [cf. Fig. 8(b)], whereas the algebraically unstable response described by Eq. (2) is formed from a single asymptotically growing peak in a region of long-time decay and transient growth [cf. Fig. 8(a)].

Although bounding x/t rays at zero growth cannot be found, the spreading character of an algebraic instability may be quantified by examining locations at which the local amplitude of the response is at some small fraction of the peak amplitude. If we take $(A + v_0) \neq 0$, then the first terms in Eqs. (9) and (10) are dominant as $t \to \infty$. Dividing the amplitude of the dominant term in Eq. (10) (omitting the cosine) by the dominant term in Eq. (9) leads to

$$R = K \left| \frac{x}{t} - c \right|^{\frac{2-3n}{2n-2}} t^{\frac{1}{n} - \frac{3}{2}}, \quad K = \frac{n^{\frac{2n-1}{2n-2}} \alpha^{\frac{3n-2}{n(2n-2)}} \sqrt{\pi(n-1)/2}}{\Gamma(1/n) \cos\left(\frac{\pi}{2n}\right)}, \tag{15}$$

where R describes the ratio of off-peak amplitudes to the peak amplitude at a specific x and t, for an x/t far enough away from the peak ($x/t = c$) such that the $t \to \infty$ asymptotic behavior has been reached (see Figs. 2 and 3). Rearranging Eq. (15) for x provides a measure of the breadth of the algebraically unstable packet at a specific R,

$$x_{R+} - x_{R-} = 2\left(\frac{K}{R}\right)^{\frac{2n-2}{3n-2}} t^{\frac{1}{n}}, \tag{16}$$

which indicates that, even though only the peak (as opposed to a region) grows as $t \to \infty$, the surrounding region of finite amplitude spreads like $t^{1/n}$. For comparison, an exponentially unstable response spreads according to $(x_+ - x_-) = (V_+ - V_-)t$ as $R \to 0$ and $t \to \infty$.

Another point of comparison is the connection between the maximum growth rate of an instability and the Fourier modes of the growing packet. For exponential instabilities, it can be shown that the

maximum of σ with respect to x/t is the same as the maximum of ω_i with respect to k_r [35]. Thus, for exponential instabilities, the maximum growth rate in the response corresponds to the one obtained from modal analysis. This maximum growth occurs at a saddle point, which corresponds to a real wave number in the observed system response. Thus, a Fourier series solution composed of real wave numbers naturally provides the correct stability conclusion for the governing PDE (i.e., one mode dominates over the others). For algebraic growth, the maximum growth rate is not tied to a specific wave number. Instead, the algebraic stability character arises from a superposition of all modes; this was first pointed out by Case [14].

IV. CONCLUSIONS

For the class of flows examined here, long-time algebraic growth is characterized by removable singularities that appear in the Fourier integral response to an impulse disturbance. These singularities preclude a straightforward use of the methods of stationary phase or steepest descent as is used in exponentially growing responses, and care must be taken to extract long-time asymptotic behaviors. This is in contrast to the Fourier integrals involving exponentially growing modes. Although the solutions of algebraically and exponentially growing responses appear to have similar features, there are some key propagation differences. For one, although both algebraic and exponential instabilities have breadth as they propagate, only exponential instabilities have long-time growth for all locations within this breadth. The peak of an algebraically unstable response is, at least for the class of problems examined here, forever surrounded by a region of transient growth that cradles the peak as time progresses. In the limit of long time, only the peak grows algebraically. The degree to which the features elucidated here are common to other algebraic instabilities is an open problem and is clearly a subject for future work.

ACKNOWLEDGMENT

APPENDIX A: ALTERNATIVE METHOD TO OBTAIN EQ. (7)

This Appendix provides an alternative approach for obtaining Eq. (7), which solely uses the Fourier transform. Taking the Fourier transform of Eq. (2) leads to

$$\frac{d^2\hat{h}}{dt^2} + 2cik\frac{d\hat{h}}{dt} + (\alpha^2 k^{2n} - c^2 k^2)\hat{h} = A\delta(t), \quad \hat{h}(0) = h_0, \quad \frac{d\hat{h}}{dt}(0) = v_0, \qquad \text{(A1)}$$

where $\hat{h}$ denotes the Fourier transform of h. Equation (A1) is a linear constant coefficient ordinary differential equation, whose solution is

$$\hat{h} = e^{-ikct}\left[h_0\cos(\alpha k^n t) + \frac{v_0 + A + ikch_0}{\alpha k^n}\sin(\alpha k^n t)\right]. \qquad \text{(A2)}$$

The inverse Fourier transform of Eq. (A2) is Eq. (7).

APPENDIX B: EVALUATION OF INTEGRALS RELEVANT TO ALGEBRAIC INSTABILITIES

This Appendix provides general formulas for the evaluation of key integrals that arise in the analysis of Eq. (2).

1. Integral formulas relevant to Eq. (2) when $\frac{x}{t} = c$

In this section, general formulas for convergent integrals of the following form are established:

$$I = \int_0^\infty \frac{\sin(ak^n)}{k^n}dk \quad \text{for } n > 0, \quad a > 0. \qquad \text{(B1)}$$

First, Eq. (B1) is differentiated with respect to a to obtain

$$\frac{dI}{da} = \int_0^\infty \cos(ak^n)\,dk. \tag{B2a}$$

Equation (B1) indicates that the following constraint must be satisfied:

$$I = 0 \quad \text{at} \quad a = 0. \tag{B2b}$$

The integral in Eq. (B2a) is provided in closed form on page 419, Eq. (3.712-2) of Ref. [46]:

$$\int_0^\infty \cos(ak^n)\,dk = \frac{\Gamma\left(\frac{1}{n}\right)\cos\left(\frac{\pi}{2n}\right)}{na^{\frac{1}{n}}}, \tag{B3}$$

where $\Gamma(\frac{1}{n})$ is the gamma function of the indicated argument. To determine I from Eq. (B2a), the right-hand side of (B3) is integrated with respect to a and Eq. (B2b) is applied to obtain

$$I = \int_0^\infty \frac{\sin(ak^n)}{k^n}dk = \left\{ \begin{array}{ll} \frac{\Gamma\left(\frac{1}{n}\right)\cos\left(\frac{\pi}{2n}\right)a^{1-\frac{1}{n}}}{n-1} & \text{for } n > 1 \\ \frac{\pi}{2}\operatorname{sgn}(a) & \text{for } n = 1 \end{array} \right\}. \tag{B4}$$

2. Integral formulas relevant to Eq. (2) when $\frac{x}{t} \neq c$

In this section, general formulas for integrals that arise when $\frac{x}{t} \neq c$ are established. The complexity of these integrals precludes a general closed-form solution, like those of Sec. B 1 for $\frac{x}{t} = c$. Thus, attention is focused on the limit of long time, t, to determine their asymptotic behaviors; this approach is sufficient to establish the morphology of algebraic growth in this paper. The following three integrals will be evaluated:

$$J = \int_0^\infty \cos(ak^nt)\cos(bkt)\,dk, \tag{B5}$$

$$K = \int_0^\infty \frac{\sin(ak^nt)\cos(bkt)}{k^n}\,dk, \tag{B6}$$

$$L = \int_0^\infty \frac{\sin(ak^nt)\sin(bkt)}{k^{n-1}}\,dk, \tag{B7}$$

where $a > 0$, $b \neq 0$, and $n \geqslant 2$ is an integer. Note that these integrals are related in a very specific way and are listed above in the order by which they may be evaluated in the limit of long time as detailed in Secs. B 2 a–B 2 c below. Note also that these integrals may be evaluated *exactly* for the case where $n = 2$ for all time, and these results are provided in Sec. B 3.

a. Evaluation of integral J in the limit of long time

To evaluate the integral J in Eq. (B5) as $t \to \infty$, the integrand is rewritten using the identity

$$\cos(ak^nt)\cos(bkt) = \tfrac{1}{2}\cos[\phi(k)t] + \tfrac{1}{2}\cos[\psi(k)t], \tag{B8a}$$

where

$$\phi(k) = bk + ak^n \quad \text{and} \quad \psi(k) = bk - ak^n. \tag{B8b}$$

With this notation, the integral J may be expressed in complex form, J', as

$$J' = \frac{1}{2}\int_0^\infty e^{i\phi(k)t}\,dk + \frac{1}{2}\int_0^\infty e^{i\psi(k)t}\,dk, \tag{B9a}$$

where

$$J = \operatorname{Real}[J']. \tag{B9b}$$

The complex integrals in Eq. (B9a) may be evaluated as $t \to \infty$ via the method of stationary phase [5] when a stationary point lies in the range of integration, since the path of integration is along the real axis, and the functions $\phi(k)$ and $\psi(k)$ are purely real. The locations of the stationary points in Eq. (B9a) occur at the k values that lead to either $\frac{d\phi}{dk} = 0$ or $\frac{d\psi}{dk} = 0$ and thus depends on the sign of b. For $b < 0$, a stationary point lies along the path of integration in $\phi(k)$ and not $\psi(k)$. For situations in which a stationary point does not lie between the limits of integration, integration by parts can be used to establish the asymptotic form; this latter method yields an $O(\frac{1}{t})$ dependence as $t \to \infty$. Applying these methods to the two integrals in Eq. (B9a) yields

$$
\int_0^\infty e^{i\phi(k)t}\, dk \sim
\left\{
\begin{array}{ll}
\left(\dfrac{2\pi}{\beta a^{\frac{1}{n-1}} t}\right)^{\frac{1}{2}} e^{i(\frac{\pi}{4} - \delta a^{\frac{1}{1-n}} t)} & \text{for } b < 0 \\[4pt]
O\left(\dfrac{1}{t}\right) & \text{for } b > 0
\end{array}
\right\},
\tag{B10a}
$$

$$
\int_0^\infty e^{i\psi(k)t}\, dk \sim
\left\{
\begin{array}{ll}
O\left(\dfrac{1}{t}\right) & \text{for } b < 0 \\[4pt]
\left(\dfrac{2\pi}{\beta a^{\frac{1}{n-1}} t}\right)^{\frac{1}{2}} e^{-i(\frac{\pi}{4} - \delta a^{\frac{1}{1-n}} t)} & \text{for } b > 0
\end{array}
\right\},
\tag{B10b}
$$

where

$$
\beta = n(n-1)\left(\frac{|b|}{n}\right)^{\frac{n-2}{n-1}} \quad \text{and} \quad \delta = (n-1)\left(\frac{|b|}{n}\right)^{\frac{n}{n-1}}.
\tag{B11a}
$$

Using (B10) in Eq. (B9), the desired asymptotic result for Eq. (B5) is obtained:

$$
J \sim \left(\frac{2\pi}{\beta a^{\frac{1}{n-1}}}\right)^{\frac{1}{2}} t^{-\frac{1}{2}} \cos\left(\frac{\pi}{4} - \delta a^{\frac{1}{1-n}} t\right) \quad \text{as } t \to \infty, \quad n \geqslant 2, \quad a > 0, \quad b \neq 0.
\tag{B11b}
$$

b. Evaluation of integral K in the limit of long time

To evaluate the integral K in Eq. (B6) as $t \to \infty$, (B5) and (B6) indicate that

$$
\frac{dK}{da} = tJ,
\tag{B12a}
$$

where by inspection

$$
K \to 0 \quad \text{at} \quad a \to 0.
\tag{B12b}
$$

Substituting (B11b) into (B12a) and integrating with respect to a, the following result is obtained:

$$
K \sim \left(\frac{\pi t}{2\beta}\right)^{\frac{1}{2}} \int_\infty^a \frac{\cos\left(\frac{\pi}{4} - \delta \xi^{\frac{1}{n-1}} t\right)}{\xi^{\frac{1}{2(n-1)}}}\, d\xi + C \quad \text{as} \quad t \to \infty,
$$

where C is an integration constant to be evaluated later. This integral is transformed via a variable substitution $s = \xi^{\frac{1}{1-n}}$ to obtain

$$
K \sim (1-n)\left(\frac{\pi t}{2\beta}\right)^{\frac{1}{2}} \int_\infty^{a^{\frac{1}{1-n}}} \frac{\cos\left(\frac{\pi}{4} - \delta s t\right)}{s^{n-\frac{1}{2}}}\, ds + C
\tag{B13a}
$$

as $t \to \infty$. The asymptotic behavior at long time may be be established via integration by parts [5], and the leading order expression for (B6) is

$$
K \sim \frac{(n-1)}{\delta}\left(\frac{\pi}{2\beta}\right)^{\frac{1}{2}} a^{\frac{n-\frac{1}{2}}{n-1}} t^{-\frac{1}{2}} \sin\left(\frac{\pi}{4} - \delta a^{\frac{1}{1-n}} t\right)
\tag{B13b}
$$

as $t \to \infty$, where (B12b) has been applied and the parameters β and δ are given in Eq. (B11a).

c. Evaluation of integral L in the limit of long time

To evaluate the integral L in Eq. (B7) as $t \to \infty$, (B6) and (B7) indicate that

$$L = -\frac{1}{t}\frac{dK}{db}. \tag{B14}$$

Taking the indicated derivative of K in Eq. (B14), using (B13b), and neglecting subdominant terms as $t \to \infty$ yields

$$\frac{dK}{db} \sim \frac{(1-n)}{\delta}\left(\frac{\pi}{2\beta}\right)^{\frac{1}{2}} a^{\frac{n-3}{n-1}} t^{\frac{1}{2}} \cos\left(\frac{\pi}{4} - \delta a^{\frac{1}{1-n}} t\right)\frac{d\delta}{db} \quad \text{as } t \to \infty, \quad n \geqslant 2, \quad a > 0, \quad b \neq 0, \tag{B15a}$$

where from Eq. (B11a)

$$\frac{d\delta}{db} = \mathrm{sgn}(b)\left(\frac{|b|}{n}\right)^{\frac{1}{n-1}}. \tag{B15b}$$

Upon substitution of (B15) into (B14), the desired result is obtained:

$$L \sim \mathrm{sgn}(b)\frac{(n-1)}{\delta}\left(\frac{\pi}{2\beta}\right)^{\frac{1}{2}} a^{\frac{n-3}{n-1}} t^{-\frac{1}{2}} \cos\left(\frac{\pi}{4} - \delta a^{\frac{1}{1-n}} t\right) \quad \text{as } t \to \infty, \quad n \geqslant 2, \quad a > 0, \quad b \neq 0. \tag{B16}$$

d. Summary of integral results relevant to $\frac{x}{t} \neq c$ as $t \to \infty$

$$\int_0^\infty \cos(ak^n t)\cos(bkt)\, dk \sim \left(\frac{\pi}{2\beta a^{\frac{1}{n-1}}}\right)^{\frac{1}{2}} t^{-\frac{1}{2}} \cos\left(\frac{\pi}{4} - \delta a^{\frac{1}{1-n}} t\right), \tag{B17a}$$

$$\int_0^\infty \frac{\sin(ak^n t)\cos(bkt)}{k^n}\, dk \sim \frac{(n-1)}{\delta}\left(\frac{\pi}{2\beta}\right)^{\frac{1}{2}} a^{\frac{n-\frac{1}{2}}{n-1}} t^{-\frac{1}{2}} \cos\left(\frac{\pi}{4} + \delta a^{\frac{1}{1-n}} t\right), \tag{B17b}$$

$$\int_0^\infty \frac{\sin(ak^n t)\sin(bkt)}{k^{n-1}}\, dk \sim \mathrm{sgn}(b)\frac{(n-1)}{\delta}\left(\frac{\pi}{2\beta}\right)^{\frac{1}{2}} a^{\frac{n-3}{n-1}} t^{-\frac{1}{2}} \cos\left(\frac{\pi}{4} - \delta a^{\frac{1}{1-n}} t\right). \tag{B17c}$$

Note that in writing (B17b), a trigonometric identity has been applied to (B13b), which accounts for the differences in form.

3. Integral formulas relevant to Eq. (2) for $n = 2$

Exact integral formulas are now provided for cases where $n = 2$ in Eqs. (B5)–(B7). Using Eq. (3.691-7) on page 415 of Ref. [46], Eq. (B5) is evaluated for $n = 2$ to yield

$$\int_0^\infty \cos(ak^2 t)\cos(bkt)\, dk = \frac{1}{2}\left(\frac{\pi}{a}\right)^{\frac{1}{2}} t^{-\frac{1}{2}} \cos\left(\frac{\pi}{4} - \frac{b^2 t}{4a}\right) \tag{B18}$$

for $a > 0$. Although restricted for $b > 0$ in Ref. [46], by inspection it is apparent that Eq. (B18) is valid for all b, and this is validated by Eq. (B3) for $b = 0$ and $n = 2$. For $n = 2$, Eq. (B6) may be

evaluated directly using Eq. (3.851-5) on page 475 of Ref. [46] to obtain

$$\int_0^\infty \frac{\sin(ak^2t)\cos(bkt)}{k^2}\,dk$$
$$= \frac{|b|\pi}{2}t\left[S\left(\frac{|b|}{2a^{\frac{1}{2}}}t^{\frac{1}{2}}\right) - C\left(\frac{|b|}{2a^{\frac{1}{2}}}t^{\frac{1}{2}}\right) \right] + (a\pi)^{\frac{1}{2}}t^{\frac{1}{2}}\cos\left(\frac{\pi}{4} - \frac{b^2t}{4a}\right) \quad \text{for} \quad a > 0, \quad \text{(B19a)}$$

where absolute values have been added to remove the constraint that $b > 0$ in Ref. [46]. The brackets in Eq, (3.851-5) of Ref. [46] are incorrectly placed and have been corrected in Eq. (B19a), and this correction makes it clear that the equation is indeed valid for all b. In (B19a), $S()$ and $C()$ are the Fresnel integrals defined in Ref. [46] (p. xxxvi) in terms of the arbitrary argument z as

$$S(z) = \sqrt{\frac{2}{\pi}}\int_0^z \sin(k^2)dk,$$

$$C(z) = \sqrt{\frac{2}{\pi}}\int_0^z \cos(k^2)dk. \quad \text{(B19b)}$$

Last, by integrating Eq. (3.691-5) on page 415 of Ref. [46] with respect to b, the following result is obtained:

$$\int_0^\infty \frac{\sin(ak^2t)\sin(bkt)}{k}dk = \frac{\pi}{2}\text{sgn}(b)\left[S\left(\frac{|b|}{2a^{\frac{1}{2}}}t^{\frac{1}{2}}\right) - C\left(\frac{|b|}{2a^{\frac{1}{2}}}t^{\frac{1}{2}}\right) \right]. \quad \text{(B20)}$$

---

[1] S. J. Weinstein and K. J. Ruschak, Coating flows, Annu. Rev. Fluid Mech. **36**, 29 (2004).

[2] G. B. Whitham, *Linear and Nonlinear Waves*, Vol. 42 (John Wiley & Sons, New York, 2011).

[3] J. Lighthill, *Waves in Fluids* (Cambridge University Press, Cambridge, UK, 2001).

[4] N. S. Barlow, B. T. Helenbrook, S. P. Lin, and S. J. Weinstein, An interpretation of absolutely and convectively unstable waves using series solutions, Wave Motion **47**, 564 (2010).

[5] C. M. Bender and S. A. Orszag, *Advanced Mathematical Methods for Scientists and Engineers I: Asymptotic Methods and Perturbation Theory* (McGraw-Hill, New York, 1978).

[6] N. Bleistein, *Mathematical Methods for Wave Phenomena* (Academic Press, Orlando, FL, 1984).

[7] Lord Rayleigh, On the stability, or instability, of certain fluid motions, Proc. Math. Soc. Lond. **11**, 57 (1880).

[8] P. J. Schmid, Nonmodal stability theory, Annu. Rev. Fluid Mech. **39**, 129 (2007).

[9] L. N. Trefethen and M. Embree, *Spectra and Pseudospectra: The Behavior of Nonnormal Matrices and Operators* (Princeton University Press, Princeton, NJ, 2005).

[10] P. J. Schmid and D. S. Henningson, Chapter 3.3: Further Results on Spectra and Eigenfunctions, in *Stability and Transition in Shear Flows* (Springer Science & Business Media, New York, 2001), pp. 85–96.

[11] M. Hirota, T. Tatsuno, S. Kondoh, and Z. Yoshida, Secular behavior of electrostatic Kelvin–Helmholtz (diocotron) modes coupled with plasma oscillations, Phys. Plasmas **9**, 1177 (2002).

[12] M. Hirota, T. Tatsuno, and Z. Yoshida, Degenerate continuous spectra producing localized secular instability: An example in a non-neutral plasma, J. Plasma Phys. **69**, 397 (2003).

[13] M. Hirota, T. Tatsuno, and Z. Yoshida, Resonance between continuous spectra: Secular behavior of Alfvén waves in a flowing plasma, Phys. Plasmas **12**, 012107 (2005).

[14] K. M. Case, Stability of inviscid plane Couette flow, Phys. Fluids **3**, 143 (1960).

[15] G. Chimonas, Algebraic disturbances in stratified shear flows, J. Fluid. Mech. **90**, 1 (1979).

[16] R. A. Smith and M. N. Rosenbluth, Algebraic Instability of Hollow Electron Columns and Cylindrical Vortices, Phys. Rev. Lett. **64**, 649 (1990).

[17] A. V. Arefiev, I. A. Kotelnikov, M. Romé, and R. Pozzoli, $l = 1$ diocotron instability of single charged plasmas, Plasma Phys. Rep. **28**, 141 (2002).

[18] V. I. Pariev and G. L. Delzanno, Stability analysis of hollow electron columns including compressional and thermal effects: Initial value treatment, Phys. Plasmas **10**, 1262 (2003).

[19] F. Volponi, Local algebraic instability of shear-flows in the Rayleigh equation, J. Phys. A **38**, 4293 (2005).

[20] D. S. Nolan and M. T. Montgomery, The algebraic growth of wavenumber one disturbances in hurricane-like vortices, J. Atmos. Sci. **57**, 3514 (2000).

[21] L. De Luca and M. Costa, Instability of a spatially developing liquid sheet, J. Fluid. Mech. **331**, 127 (1997).

[22] P. Luchini, Is a plane liquid curtain algebraically absolutely unstable? Phys. Fluids **16**, 2154 (2004).

[23] N. S. Barlow, B. T. Helenbrook, and S. P. Lin, Transience to instability in a liquid sheet, J. Fluid. Mech. **666**, 358 (2011).

[24] Sung Lin, *Breakup of Liquid Sheets and Jets* (Cambridge University Press, New York, 2003).

[25] If written as a first order system in time when the equation is discretized in space.

[26] S. Davis, Interfacial fluid dynamics, in *Perspectives in Fluid Dynamics*, edited by G. K. Batchelor, H. K. Moffatt, and M. G. Worster (Cambridge University Press, Cambridge, UK, 2000), pp. 1–49.

[27] S. C. Mohapatra and T. Sahoo, Surface gravity wave interaction with elastic bottom, Appl. Ocean Res. **33**, 31 (2011).

[28] P. Huerre, Open shear flow instabilities, in *Perspectives in Fluid Dynamics*, edited by G. K. Batchelor, H. K. Moffatt, and M. G. Worster (Cambridge University Press, Cambridge, UK, 2000), pp. 159–229.

[29] P. J. Schmid and D. S. Henningson, Chapter 7.2: Absolute Instability, in *Stability and Transition in Shear Flow* (Springer Science & Business Media, New York, 2001), pp. 270–284.

[30] P. Huerre and M. Rossi, Hydrodynamic instabilities in open flows, in *Hydrodynamics and Nonlinear Instabilities*, edited by C. Godrèche and P. Manneville (Cambridge University Press, New York, 1998), pp. 81–288.

[31] J. J. Stoker, *Water Waves: The Mathematical Theory with Applications* (John Wiley & Sons, New York, 1957).

[32] A. Clarke, S. J. Weinstein, A. G. Moon, and E. A. Simister, Time-dependent equations governing the shape of a two-dimensional liquid curtain, part 2: Experiment, Phys. Fluids **9**, 3637 (1997).

[33] M. J. Lighthill, *Introduction to Fourier Analysis and Generalised Functions* (Cambridge University Press, Cambridge, UK, 1962).

[34] N. S. Barlow, S. J. Weinstein, and B. T. Helenbrook, On the response of convectively unstable flows to oscillatory forcing with application to liquid sheets, J. Fluid. Mech. **699**, 115 (2012).

[35] N. S. Barlow, B. T. Helenbrook, and S. J. Weinstein, Algorithm for spatio-temporal analysis of the signaling problem, IMA J. Appl. Math. (2015), doi: 10.1093/imamat/hxv040.

[36] B. T. Helenbrook and N. S. Barlow, Spatial-temporal stability analysis of faceted growth with application to horizontal ribbon growth, J. Crys. Growth **454**, 35 (2016).

[37] P. M. Morse and H. Feshbach, *Methods of Theoretical Physics* (McGraw-Hill, New York, 1953).

[38] H. F. Weinberger, *A First Course in Partial Differential Equations* (Xerox College Publishing, Lexington, MA, 1965).

[39] D. E. Ashpis and E. Reshotko, The vibrating ribbon problem revisited, J. Fluid. Mech. **213**, 531 (1990).

[40] J. M. Gordillo and M. Pérez-Saborid, Transient effects in the signaling problem, Phys. Fluids **14**, 4329 (2002).

[41] A continuous dispersion relation $\omega(k)$ is sufficient but not necessary for a continuous spectrum of saddles and a continuous $\sigma = f(x/t)$. One example of a discontinuous dispersion relation leading to a continuous $\sigma = f(x/t)$ is given in Ref. [34] .

[42] C. Cossu and J. M. Chomaz, Global Measures of Local Convective Instabilities, Phys. Rev. Lett. **78**, 4387 (1997).

[43] R. E. Hunt and D.G. Crighton, Instability of flows in spatially developing media, Proc. R. Soc. Lond. A **435**, 109 (1991).

[44] R. J. Briggs, *Electron-Stream Interaction with Plasmas* (MIT Press, Cambridge, MA, 1964).

[45] P. Schmidt, L. Ó Náraigh, M. Lucquiaud, and P. Valluri, Linear and nonlinear instability in vertical counter-current laminar gas-liquid flows, Phys. Fluids **28**, 042102 (2016).

[46] I. S. Gradshteyn and I. M. Ryzhik, Chapters 2.5-2.6: Trigonometric Functions, in *Table of Integrals, Series, and Products*, 7th ed., edited by A. Jeffrey and D. Zwillinger (Academic Press, Burlington, MA, 2007), pp. 390–525.